Title
Investigation of Neutron Scattering for a Multisphere Spectrometer

Author
Sun, R.-K.S.

Publication Date
1989-08-01

UC-406
LBL-27832
Preprint

Lawrence Berkeley Laboratory
UNIVERSITY OF CALIFORNIA

OCCUPATIONAL HEALTH DIVISION

Submitted to Health Physics Journal

Investigation of Neutron Scattering for a Multisphere Spectrometer

R.-K. S. Sun

August 1989

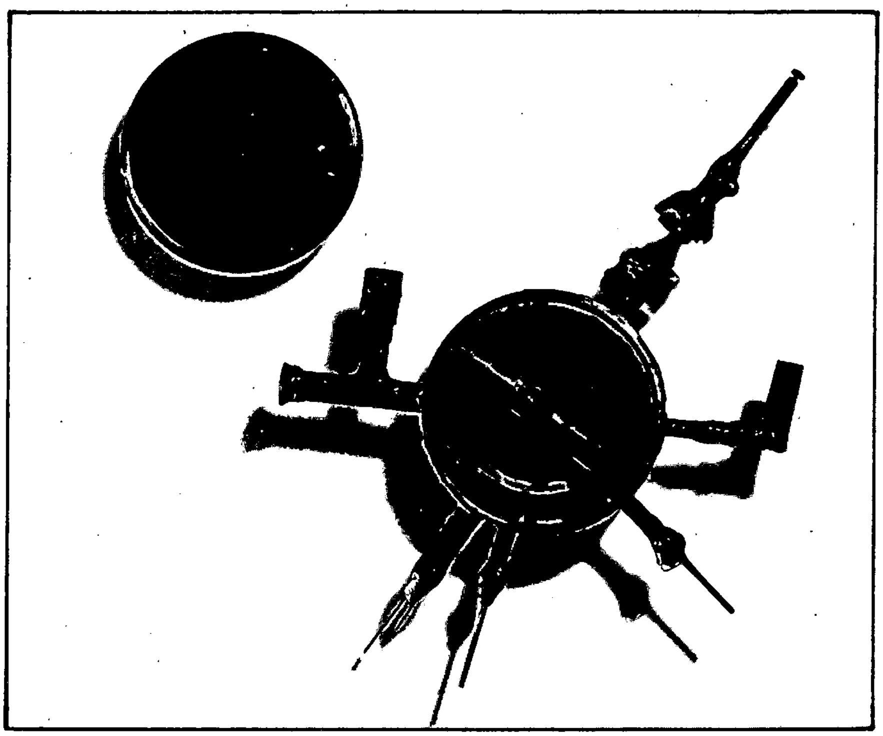

Prepared for the U.S. Department of Energy under Contract Number DE-AC03-76SF00098.

INVESTIGATION OF NEUTRON SCATTERING FOR A MULTISPHERE SPECTROMETER

Rai-Ko S. Sun

Occupational Health Division

Lawrence Berkeley Laboratory

1 Cyclotron Road

Berkeley, CA 94720

ABSTRACT

Count rates were measured as a function of distance from a planar concrete reflector for a set of 8 Bonner-sphere detectors and 4 isotopic neutron sources. These data can be used to determine the contributions of scattered neutron to the response of moderated detectors used in environments bounded by concrete. A model based on "images" of the original source can be developed to produced an equation that describes the data well, if the strengths of the image sources can be treated as variable parameters. Values of the parameters appearing in the equation are given based on least-squares analysis of the experimental results.

September 11, 1989

INVESTIGATION OF NEUTRON SCATTERING FOR A MULTISPHERE SPECTROMETER

Rai-Ko S. Sun

Occupational Health Division

Lawrence Berkeley Laboratory

1 Cyclotron Road

Berkeley, CA 94720

1.0 INTRODUCTION

An important consideration in the measurement of neutron fluence, or its dose equivalent, is neutron scattering of neutrons by the floor, ceiling, and surrounding walls, if these are of high density material, for example concrete. Neutron scattering has been investigated for some special cases [Eis65, McC76, Jen80, McC83, Jen83, Li84]. The primary purpose of those studies was to determine the contribution of scattered neutrons to the total flux density at any point within an enclosed experimental area, where a radiation detector was located and was calibrated by means of a standard neutron source. If the neutron scattering inside the experimental area is known, corrections to the neutron fluence in relation to the calibration can be made.

Since the response of detectors with spheres of various size is energy dependent, the response of the individual detectors of a multisphere spectrometer to neutron scattering will vary widely. This effect was investigated using point neutron sources and detectors in an open field over a concrete floor. The experimental data are compared with the theoretical calculation based on an image method.

2.0 MODEL FOR INVESTIGATION

In calibrating neutron detectors, the scattered radiation reaching the detector must be considered. Estimating the albedo component from the experimental result, however, is quite involved. Eisenhauer suggested a simplified "image" method for the case of a point source and a point detector located above a slab [Eis65], and Jenkins further extended this concept for simplifying the calculation of ground-scattering neutrons above a concrete surface without relying on albedo data [Jen80]. In our case, the image method was adopted, with the measurements made in an open field over a concrete reflecting plane. The horizontal distance between a monoenergetic neutron source and a detector is *D*, the vertical distance between the neutron source and the detector is *V* and the vertical distance of the source above the ground is *H*, (see Fig. 1). At the detector, the neutron fluence density due to the neutron source, ϕ_o, is proportional to its emissivity, ξ_o, and to the inverse square of the distance, r_o, between the detector and the source. The total fluence density, ϕ_t, is the sum of two components: ϕ_o, the neutrons coming directly from the neutron source, and ϕ_i, the scattered neutrons corresponding to an image with an emissivity ξ_i at a distance of r_i from the detector. In general $\xi_i \le \xi_o$. An expression for the total flux density at the detector can thus be written as

$$\phi_t = \phi_o + \phi_i, \qquad (1)$$

or

$$\phi_t = \frac{1}{4\pi} \times \left[\frac{\xi_o}{r_o^2} + \frac{\xi_i}{r_i^2}\right]. \qquad (2)$$

For a general expression of scattering resulting from *n* reflecting planes, Eqs. (1) and (2) can be modified to Eqs. (1A) and (2A), respectively:

$$\phi_t = \phi_o + \sum_{i=1}^{i=n} \phi_i, \qquad (1A)$$

and

$$\phi_t = \frac{1}{4\pi} \times \left[\frac{\xi_o}{r_o^2} + \sum_{i=1}^{i=n} \frac{\xi_i}{r_i^2}\right]. \qquad (2A)$$

From Fig. 1 we see that

$$r_o = \sqrt{D^2 + V^2} \quad \text{and} \quad r_i = \sqrt{D^2 + (2H + V)^2} \ .$$

By substitution into Eq. (2), the following is obtained:

$$\phi_t = \frac{1}{4\pi} \times \left[\frac{\xi_o}{D^2 + V^2} + \frac{\xi_i}{D^2 + (2H \pm V)^2} \right] , \tag{3}$$

where the second term in the equation is the scattered component.

2.1 ENERGY-INDEPENDENT DETECTOR

For an energy-independent detector, the measured response A_{jt} will be proportional to the quantity ϕ_t, which consists of two components: a response, A_{jo}, due to direct neutrons and another, A_{ji}, due to scattered neutrons. Therefore,

$$A_{jt} = A_{jo} + A_{ji} , \tag{4}$$

and the ratio of the measured response A_{jt} to its component A_{jo} can be expressed as

$$\frac{A_{jt}}{A_{jo}} = 1 + \frac{\xi_i}{\xi_o} \times \left[\frac{D^2 + V^2}{D^2 + (2H + V)^2} \right] = 1 + \frac{\xi_i}{\xi_o} \times \left[\frac{r_o}{r_i} \right]^2 . \tag{5}$$

The percentage of the scattered component of the response, η_{sct}, in terms of the direct component can be written as follows :

$$\eta_{sct} = \frac{A_{ji}}{A_{jo}} \times 100 = \frac{\xi_i}{\xi_o} \times \left[\frac{D^2 + V^2}{D^2 + (2H + V)^2} \right] \times 100 . \tag{6}$$

If it is assumed that there is no absorption of neutrons in the concrete, $\xi_i = \xi_o$, (never true in practice), two very simple cases can be considered with one point source and one detector.

Case 1: The point source and the detector are at the same horizontal level; hence, $V = 0$. Let $H = kD$ where k is a constant of proportionality. From Eq. (3), we then have

$$\eta_{sct} = \frac{A_{ji}}{A_{jo}} \times 100 = \left[\frac{1}{1 + (2\,k)^2} \right] \times 100. \tag{7}$$

Case 2: The point source is directly above the detector; hence $D = 0$ and V is negative. Let $H = mV$, where m is also a constant of proportionality. The percentage of scattering is now

$$\eta_{sct} = \frac{A_{ji}}{A_{jo}} \times 100 = \left[\frac{1}{(2m - 1)^2} \right] \times 100 \tag{8}$$

For example, if the proportionality constants, k in Eq. (7) and m in Eq. (8), equal 5, the value of η_{sct} will be about 1% in both cases, which means that if the height of the point source from the ground is 5 times the separation between the source and the detector, the scattered component is about 1% of the total fluence. Two sets of curves are given in Figs. 2 and 3 to illustrate Cases 1 and 2, respectively. In real situations, $\xi_i \neq \xi_o$; therefore, the idealized curves of Figs. 2 and 3 will overestimate the measured values for $\xi_i < \xi_o$ and underestimate for $\xi_i > \xi_o$.

2.1.1 COMPARISON WITH PREVIOUS EXPERIMENTAL DATA

In a previous experiment [McC76], a detector system with a second moderated BF_3 detector, which is approximately energy independent over 20 keV to 20 MeV, was suspended 1 m beneath a monoenergetic neutron point source of ^{238}PuB. This detector-source combination was raised by a crane so that counting data could be collected at various positions up to 9.14 m (30 ft) above an extensive concrete floor. The measured detector responses in counts per minute (cpm) are plotted against the distance between the source and floor, as shown by the circles in Fig. 4. This detector-source combination is described by our Case 2. When the distance between the source and floor is 9.14 m, the scattering is estimated to be 0.34 %, which may be considered as essentially zero. Using the data of that point as a reference value, i.e. $A_{jo} = 2.2 \times 10^4$ cpm as indicated by the dashed line, a curve for the total response A_{jt} that is a good fit to measured points can be calculated by using Eqs. (4) and (8). This comparison, therefore, justifies the assumption that $\xi_i < \xi_o$ for the detector-source combination.

2.2 ENERGY-DEPENDENT DETECTORS

Neutron sources are generally not monoenergetic and produce spectrum of neutrons of energy E. Therefore, the flux densities in Eq. (1) should be replaced with $d\phi_o/dE$ and $d\phi_i/dE$, respectively, which are neutron-fluence energy spectra. Similarly, the terms A_{jo} and A_{ji} of Eq. (4) can be modified to give

$$A_{jo} = \int_{E_{min}}^{E_{max}} K_j(E)\, \phi_o(E)\, dE \qquad (9)$$

and

$$A_{ji} = \int_{E_{min}}^{E_{max}} K_j(E)\,\phi_i(E)\,dE \quad , \tag{10}$$

respectively. The term $K_j(E)$ is an analytical response function of the detector j. A general expression for scattering resulting from n reflecting planes can be written as

$$A_{jt} \;=\; A_{jo} \;+\; \sum_{i=1}^{i=n} A_{ji} \quad . \tag{11}$$

3.0 EXPERIMENT USING MULTISPHERE DETECTORS

The main purpose of the experiment was to investigate the scattering effect on the responses of detectors of a multisphere spectrometer of LBL's Department of Environmental Health & Safety,. The experiment was carried out in Building B76A using 4 cylindrical neutron sources of (No. 632 PuBe, No. 633 PuLi, No. 634 PuB and No. 651 PuB) and 8 Bonner-sphere detectors. The detectors consisted of cylindrical LiI (Eu) scintillation crystals (12.7 mm in diameter × 12.7 mm high), enriched to 99% ^{6}Li, surrounded by spherical polyethylene neutron moderators ranging in diameter from 0 (bare detector) to 45.72 cm. These detectors were coupled through photomultiplier tubes and an 8-input mixer-router to a 4096-channel multichannel analyzer (MCA). Measurements were made with the sources and detectors set at the same height. For the detectors with large polyethylene spheres, i.e. 20.32, 25.5, 30.48, and 47.72 cm, the measurements were made using 1 neutron source and 1 detector at a time; for the detectors with small diameters, i.e. 0, 5.08, 7.62, and 12.5 cm, the measurements were made using 1 neutron source and 4 detectors simultaneously.

Two aluminum support frames were used. One frame supported the large detector in the middle and with the source mounted on an arm extended about 1 m to one side. The axis of the detector's cylindrical LiI (Eu) scintillation crystal was oriented in the central hole of the polyethylene sphere so that it was parallel to the axis of the source's cylindrical capsule. The center of the detector sphere and the center of the neutron source were at the same height, and the distance between these two centers was exactly 1 m. Another square frame of aluminum rod held the neutron source at the center and equidistant from each of 4 detectors mounted at the corners. Again, the center of the source and the centers of the detectors were at exactly the same height, and the distance between the source center and detectors' centers was exactly 1 m. The frames could be raised by a crane to change the distance between the detector-source combination and the concrete floor from about 0.5 m to 5 m. Data were taken with the MCA from the integral counts under a neutron peak within a given time interval and were printed out automatically. All data were converted to counting rates for further evaluation, and they are given in the Appendix.

4.0 RESULTS AND DISCUSSION

The data are grouped according to the 8 detectors, i.e. with spheres of diameters 0 (bare), 5.08, 7.62, 12.7, 20.32, 25.4, 30.48, and 45.72 cm, (0, 2, 3, 5, 8, 10, 12 and 18 in.). Each detector group has 4 sets of data from 4 neutron sources: ^{238}PuBe (No. 632), ^{238}PuLi (No. 633), ^{238}PuB (No. 634), and ^{238}PuF (No. 651).

Within each detector data set, the data from a given neutron source are normalized by a factor selected as the counting rate for nonscattering. There are 4 different normalizing factors for 4 sets of data for each detector, and the value corresponding to nonscattering response is then equal to 1. These normalizing factors are so selected that all data from the same detector would fall within a zone that may be considered as a curve with error tolerance. These data are shown in Figs. 5 to 12, where a dashed curve calculated from Eq. (5), with $\xi_i = \xi_o$, is shown for comparison with the experimental points. The normalized values of the measured responses agree with the calculated curve very well for the detector with a sphere of 12.7 cm (Fig. 8) but not for the other detectors. Since in air a reflected neutron can only lose energy, the measured responses due to scattering for detectors with large spheres, i.e. ≥ 12.7 cm (5 in.), tend to decrease with energy because of the energy dependence of the moderated detector. This is shown in Figs. 9 through 12, in which the values of the normalized responses in the low-energy region decrease as the diameter of the sphere increases.

Detectors with no sphere (bare) or with a small-diameter sphere, i.e. ≤ 7.62 cm (3 in.), are sensitive in the low energy region. The direct neutrons as well as the reflected neutrons will moderate to neutrons of lower energies, which could then be detected by bare detector or detectors with small spheres. Under these circumstances the scattering based upon simple specular reflection no longer applies. The normalized measured data are far beyond the theoretical curve for distances less than 2 m, as can be seen in Figs. 5, 6 and 7. The normalized responses of the detector with a 45.72 cm sphere (Fig. 12) do not fall within a error zone, as do those in the other figures. The apparent spread among these data can be ascribed to the low counting statistics associated with neutron sources PuF (632) and PuLi (633).

The dashed curve was obtained with the assumptions that $\xi_i = \xi_o$. In reality, the ratio of emissivities ξ_i to ξ_o can not always be equal to 1 for different moderated detectors. The theoretical formula, Eq. (5), could be modified to an empirical one by treating the ratio of emissivities as a modification factor $\alpha = \xi_i / \xi_o$ to account for the energy-dependence effect as well as the albedo. The chosen values for α are 16.95, 5.55, 1.78, 1.0, 0.7, 0.6, 0.526, and 0.4 for detectors with spheres of diameter 0 (bare), 5.08, 7.62, 12.7, 20.32, 25.4, 30.48, and 45.72 cm, respectively. In Figs. 5 – 7 and 9 – 12, a solid curve is calculated with the given value α, which is shown to be in reasonably good agreement with the measured responses of the detectors. The reciprocal of the modification factor, $1/\alpha = \xi_o / \xi_i$, increases as the diameter of the sphere, D, increases. The plot in Fig. 13 shows the value of $1/\alpha$ as a function of D. Those points, except the one for the bare detector, can be approximated by a parabola:

$$D = 4.83 + 7.12 \times \left[\frac{\xi_o}{\xi_i}\right]^2, \tag{12}$$

as show by the solid curve. Since in Eq. (12), the value of α can be evaluated as

$$\alpha = \frac{\xi_i}{\xi_o} = \sqrt{\frac{7.12}{D - 4.83}} = \frac{2.67}{\sqrt{D - 4.83}}, \tag{13}$$

it is, therefore, possible to rewrite Eq. (5) in the form of an empirical equation:

$$\frac{A_{jt}}{A_{jo}} = 1 + \alpha \times \left[\frac{r_o}{r_i}\right]^2 = 1 + \frac{2.67}{\sqrt{D - 4.83}} \times \left[\frac{r_o}{r_i}\right]^2. \tag{14}$$

This equation is valid for all the detectors with moderating spheres of the multisphere spectrometer and can be used to obtain a comparatively accurate estimate of scattering for this system.

5.0 CONCLUSION

In Figs. 8 through 11, data on moderated detectors of diameters ranging from 5 to 12 in. are shown to fall within a zone that follows closely the trend of a calculated curve based upon the image method, with a suitable modification factor in the equation.

As shown in Figs. 5 and 7, the experimental data of 3 detectors, i.e. bare, 5.08 and 7.62 cm, can not be predicted with the theoretical method, without the modification factor A, and their deviations are mainly caused by the scattered neutrons and their albedo effect. For the 45.72 cm detector, the counting statistics are poor, because the moderator absorbs so many neutrons, and the data may not be useful for analysis. However, the detectors with the 0 (bare) and 5.08 cm sphere are primarily sensitive to neutrons of energy below 10^{-2} MeV, and the detector with the 45.72 cm sphere is only sensitive to neutrons in the range of about 5 to 100 MeV. Moreover, since the counting rates of those three detectors are, in general, much smaller than those of other detectors their contributions to the dose equivalent is relatively small and can be ignored. It is, therefore, reasonable to use the simple image method, i.e. without the modification factor $\alpha = \xi_i/\xi_o$ in Eq. (5), for a quick estimate of the scattering effect on the multisphere spectrometer. An advantage of this method for dealing with an experimental area surrounded with walls and a ceiling is that the total scattering can be obtained by simple arithmetic addition by steps of the scatterings from various surfaces of reflection. The albedo effect is important for the neutron scattering, which needs further study with a MORSE computer code in the future.

In conclusion, this method shows the consistency of source data; therefore, it is useful for choosing sources for unfolding source spectra and for calibrating other detectors.

6.0 ACKNOWLEDGEMENTS

The author expresses his gratitude to individuals at Lawrence Berkeley Laboratory whose efforts were instrumental in making these measurements possible, in particular, T.M. de Castro for his careful thought and design of an elevating system for the large spheres; R.W. Yow for the construction of a crane in Building B75A, and to H.J. Jelonek and M.T. Lasartemay for frequent help throughout the experiments. The author wishes also to thank J.B. McCaslin for his thoughtful suggestion regarding the scattering experiment on Bonner spheres, W.P. Swanson for his valuable advice and comments, and R.H. Thomas and J. Young for their support and encouragement.

This work was supported by the U.S. Department of Energy under Contract No. DE-AC03-76SF00098 with the University of California.

REFERENCES

Eis65 C. Eisenhauer, "An image source technique for calculating reflection of gamma rays or neutrons," Health Phys. 11, pp. 1145-1154 (1965).

Jen80 T. M. Jenkins, "Simple recipes for ground scattering in neutron detector calibration," Health Phys. 39, pp. 41-47 (1980).

Li84 L. Li, "Reflection of ^{252}Cf fission neutrons from a concrete floor," Radiation Protection Dosimetry 5, No. 4, pp. 227-231 (1984)

McC76 J. B. McCaslin and L. D. Stephens, "Effect of neutron scattering on the calibration of moderated BF_3 detectors," Lawrence Berkeley Laboratory, Health Physics Department Internal Note HPN 57, December 22, 1976.

McC83 J. B. McCaslin, L. D. Stephens, and R. H. Thomas, "Ground scattering contribution in neutron calibrations," (Letter to the Editor), Health Phys. 44, pp. 437-439 (1983).

Jen83 T. M. Jenkins, "Reply to McCaslin, Stephens and Thomas," (Letter to the Editor), Health Phys. 44, p. 439 (1983).

FIGURE CAPTIONS

Fig. 1. Relationship of detector M to source S and its image S'.

Fig. 2. Scattering of neutrons with detector M and source S located at the same level.

Fig. 3. Scattering of neutrons with source S located on top of detector M.

Fig. 4. Scattering of neutrons with a neutron source ^{238}PuB 1 m above the detector BF_3 [McC76].

Fig. 5. Normalized scattering of neutrons for detector No. 1 (bare) and 4 sources (detector and source 1 m apart and at the same height).

Fig. 6. Normalized scattering of neutrons for detector No. 2 (5.08 cm) and 4 sources (detector and source 1 m apart and at the same height).

Fig. 7. Normalized scattering of neutrons for detector No. 3 (7.62 cm) and 4 sources (detector and source 1 m apart and at the same height).

Fig. 8. Normalized scattering of neutrons for detector No. 4 (12.70 cm) and 4 sources (detector and source 1 m apart and at the same height).

Fig. 9. Normalized scattering of neutrons for detector No. 5 (20.32 cm) and 4 sources (detector and source 1 m apart and at the same height).

Fig. 10. Normalized scattering of neutrons for detector No. 6 (25.40 cm) and 4 sources (detector and source 1 m apart and at the same height).

Fig. 11. Normalized scattering of neutrons for detector No. 7 (30.48 cm) and 4 sources (detector and source 1 m apart and at the same height).

Fig. 12. Normalized scattering of neutrons for detector No. 8 (45.72 cm) and 4 sources (detector and source 1 m apart and at the same height).

Fig. 13. Ratio of emissivities, ξ_o to ξ_i, as functions of sphere diameter, D.

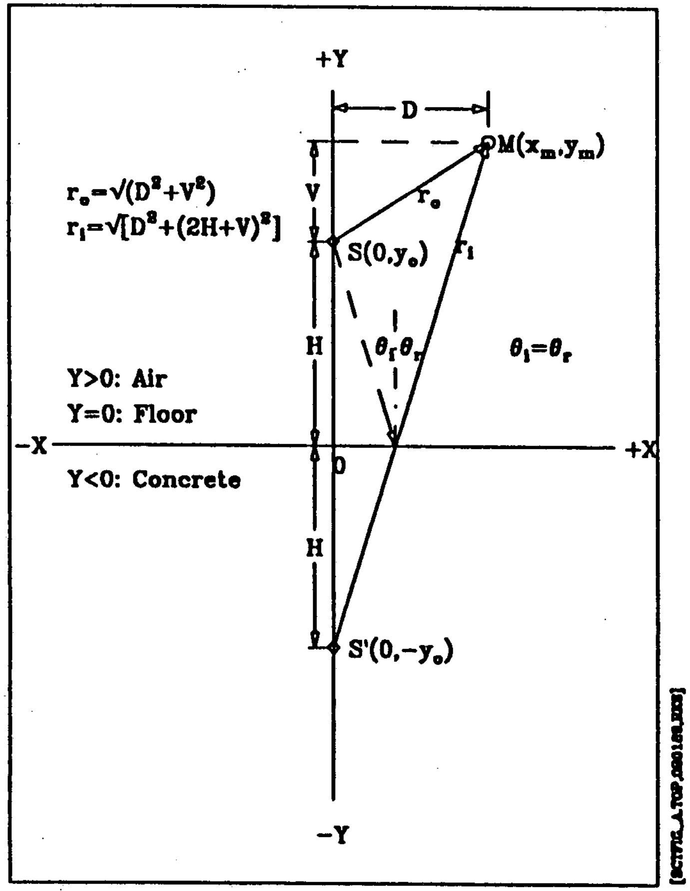

Fig. 1 Relationship of the detector M to a source S and its image S'

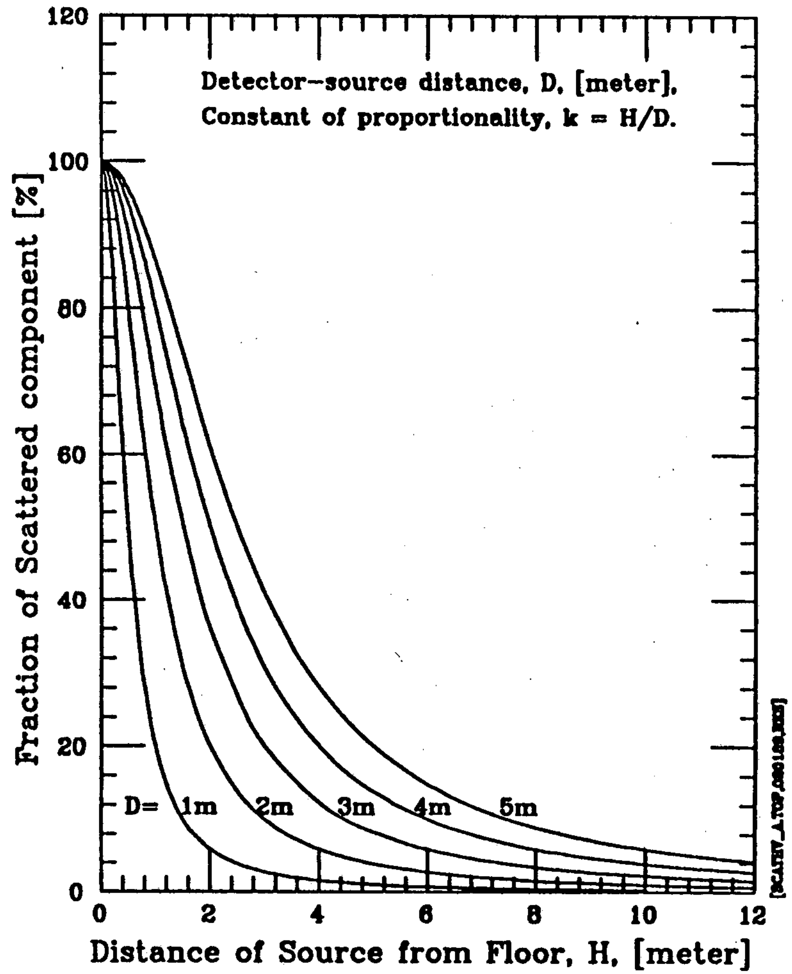

Fig. 2 Scattering of neutrons with detector M and source S at the same level.

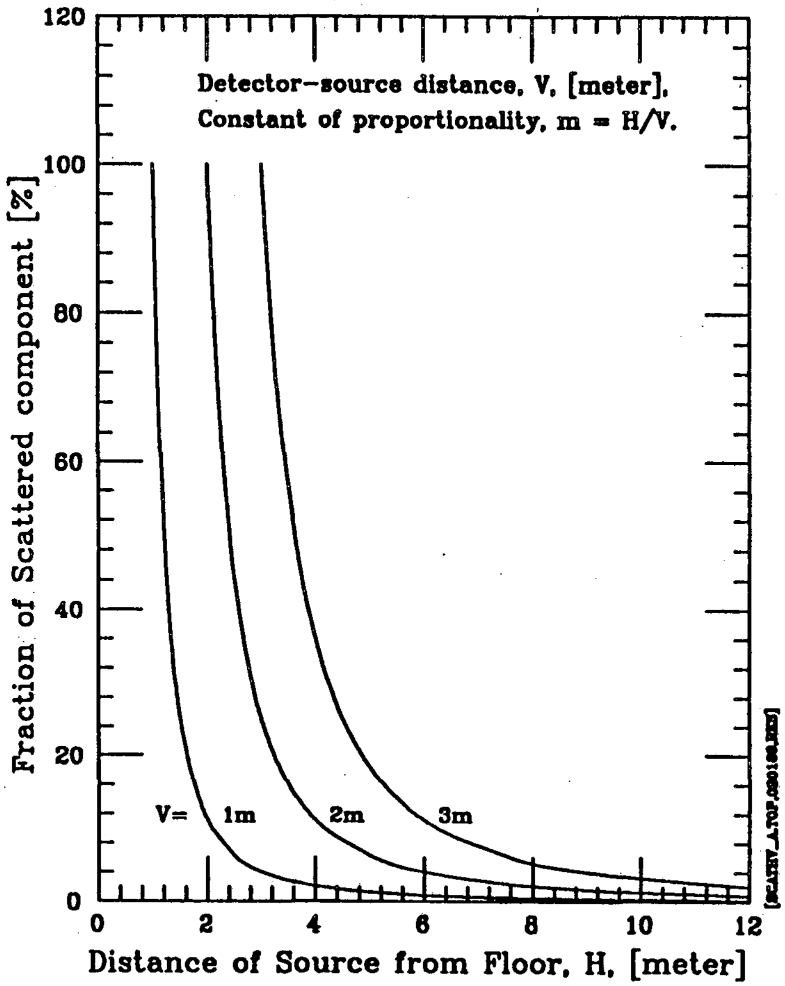

Fig. 3 Scattering of neutrons with source S on top of detector M.

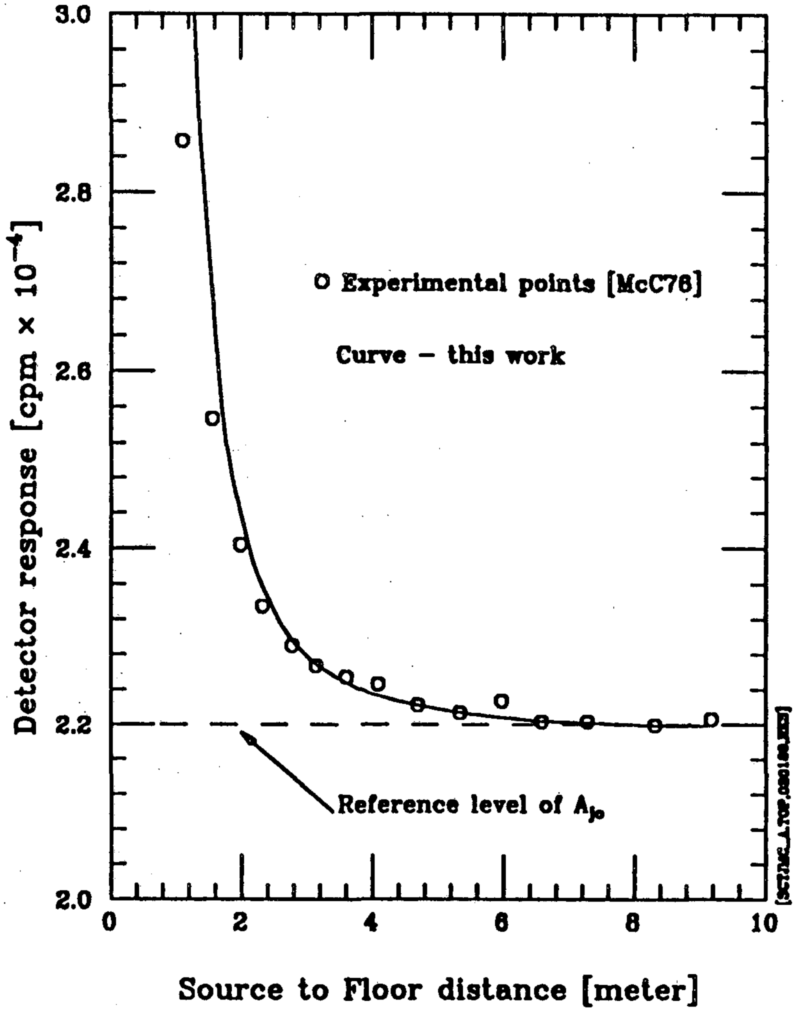

Fig. 4 Scattering of neutrons with a neutron source ^{238}PuB 1 m above the detector BF_3 [McC76]

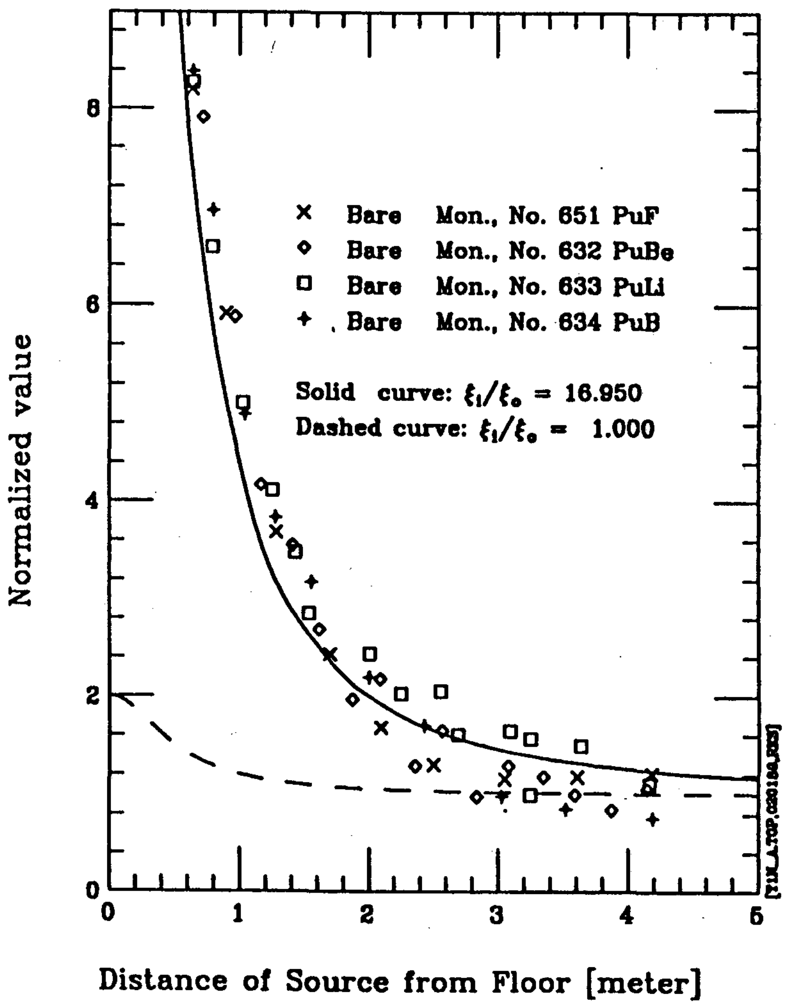

Fig. 5 Normalized scattering of neutrons for detector No. 1 (Bare) and 4 sources (detector and source is 1 m apart and at the same height).

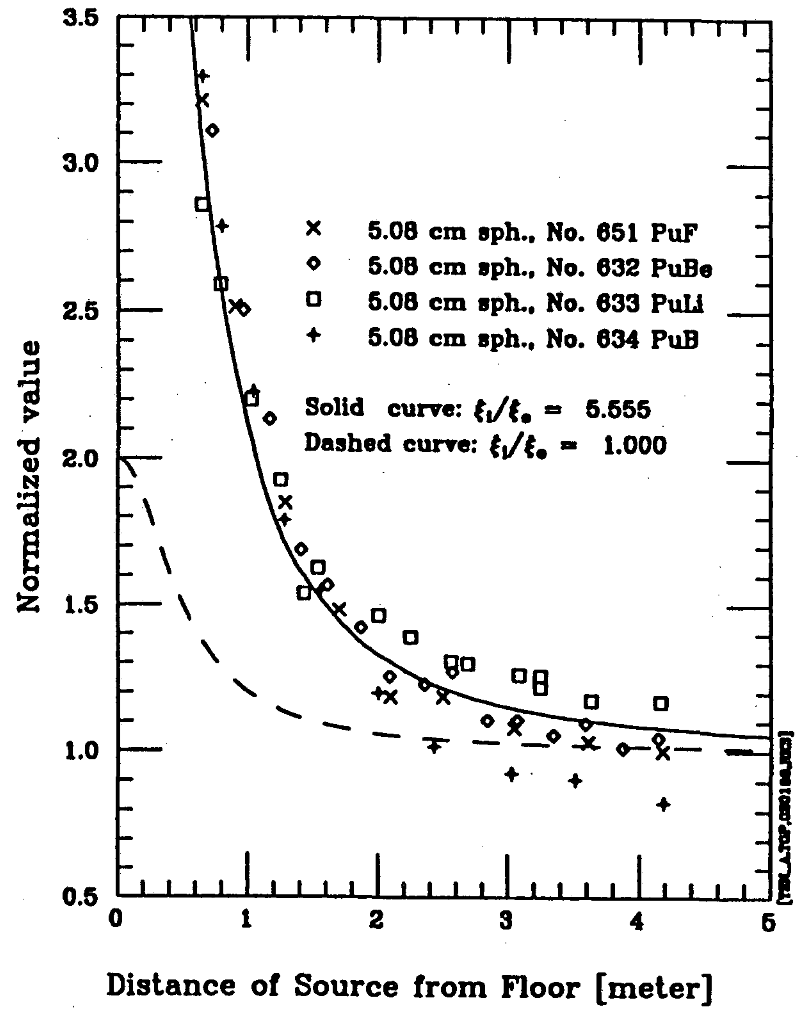

Fig. 6 Normalized scattering of neutrons for detector No. 2 (5.08 cm) and 4 sources (detector and source is 1 m apart and at the same height).

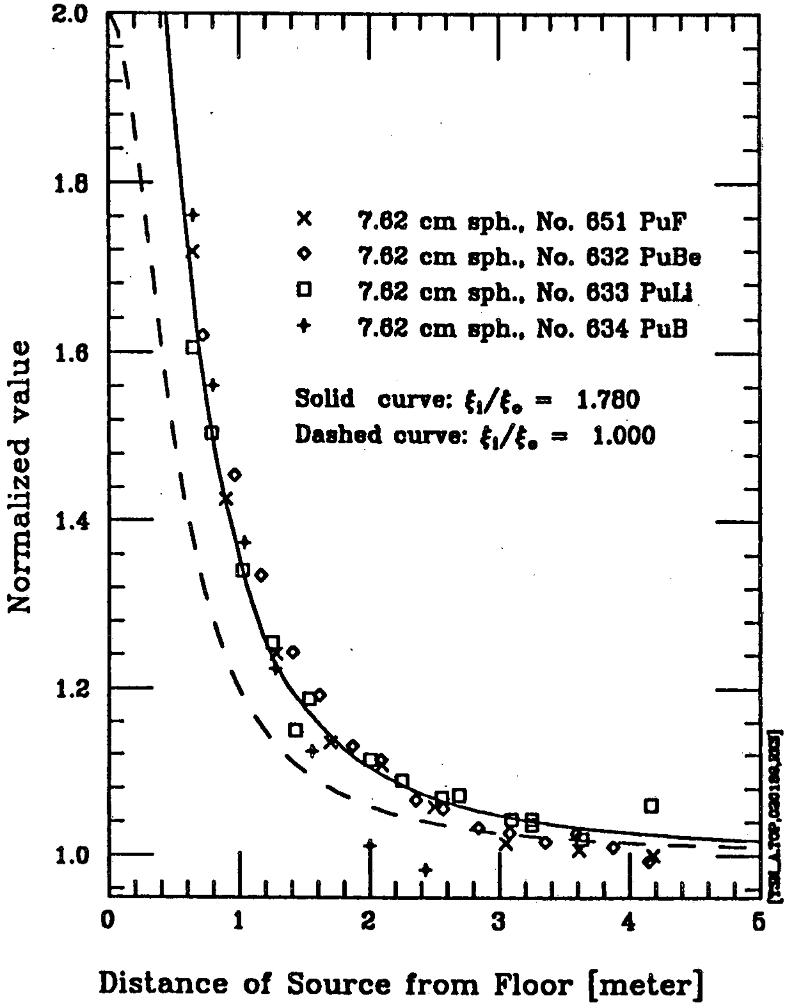

Fig. 7 Normalized scattering of neutrons for detector No. 3 (7.62 cm) and 4 sources (detector and source is 1 m apart and at the same height).

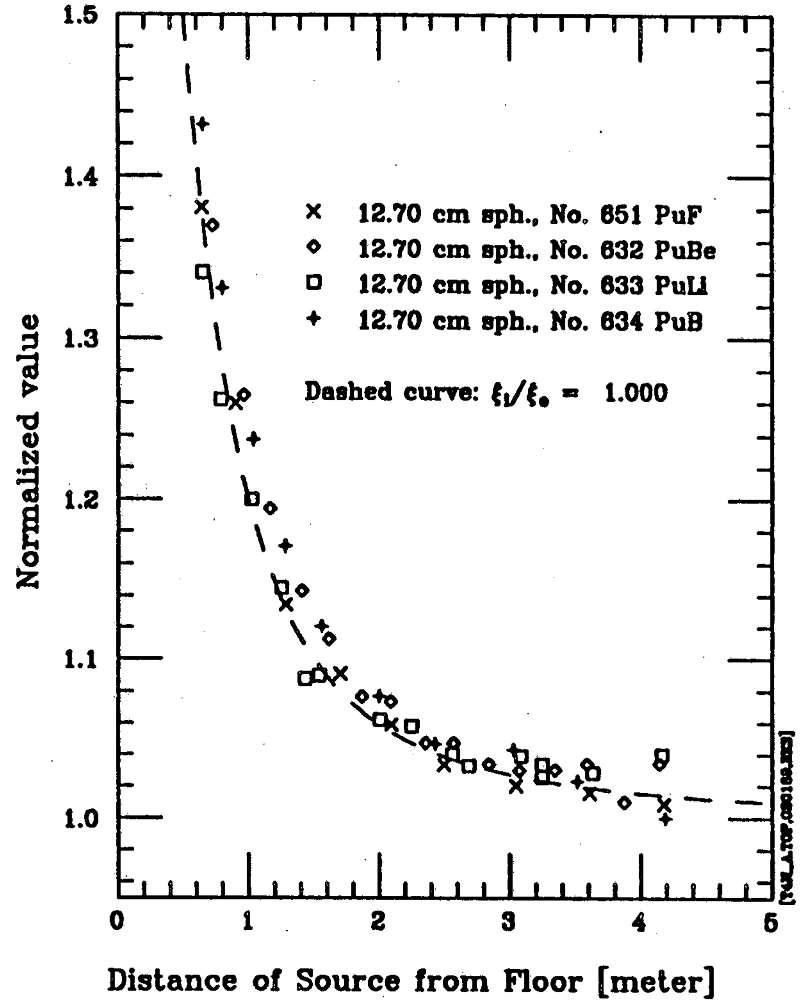

Fig. 8 Normalized scattering of neutrons for detector No. 4 (12.70 cm) and 4 sources (detector and source is 1 m apart and at the same height).

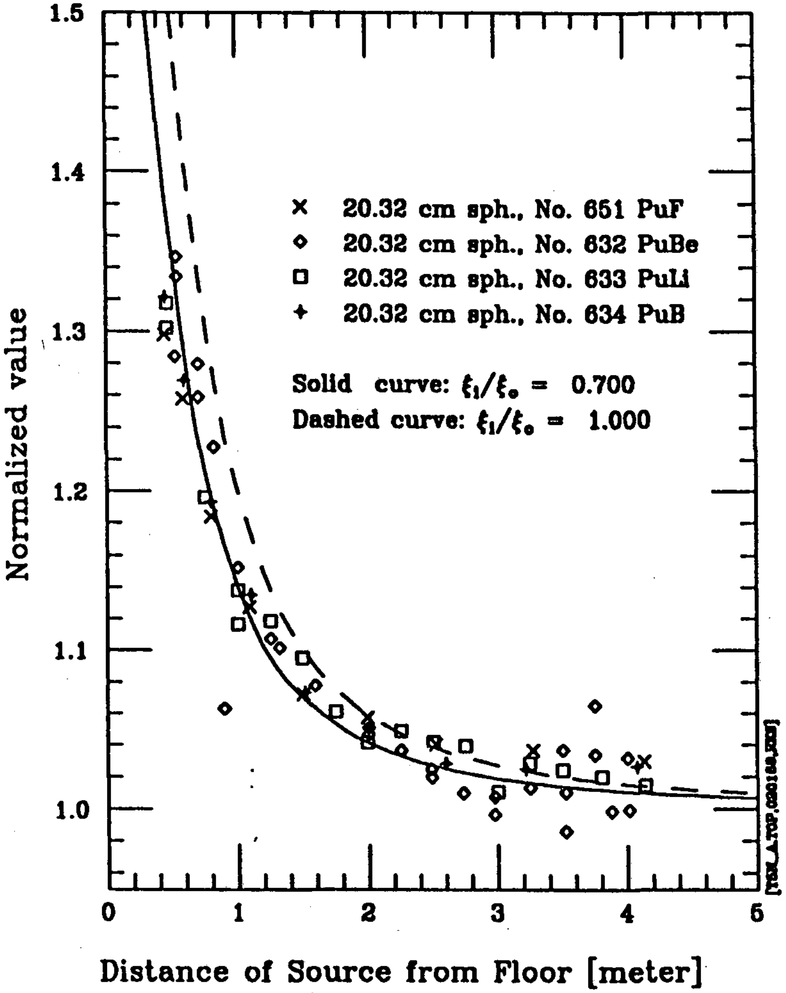

Fig. 9 Normalized scattering of neutrons for detector No. 5 (20.32 cm) and 4 sources (detector and source is 1 m apart and at the same height).

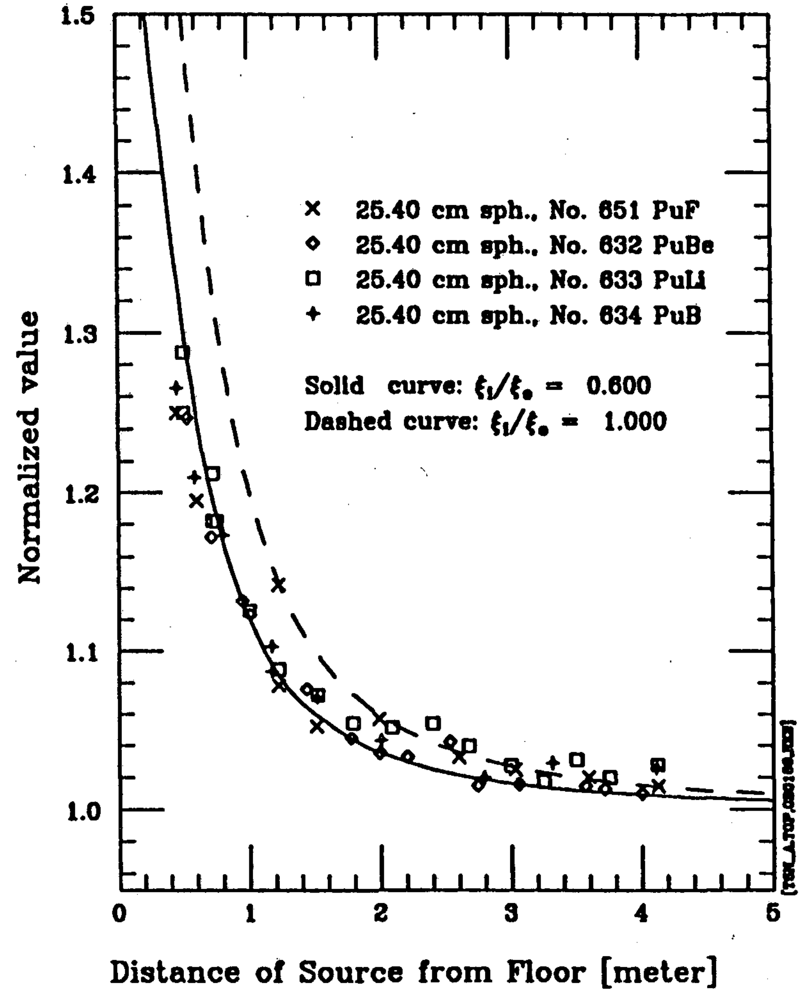

Fig. 10 Normalized scattering of neutrons for detector No. 6 (25.40 cm) and 4 sources (detector and source is 1 m apart and at the same height).

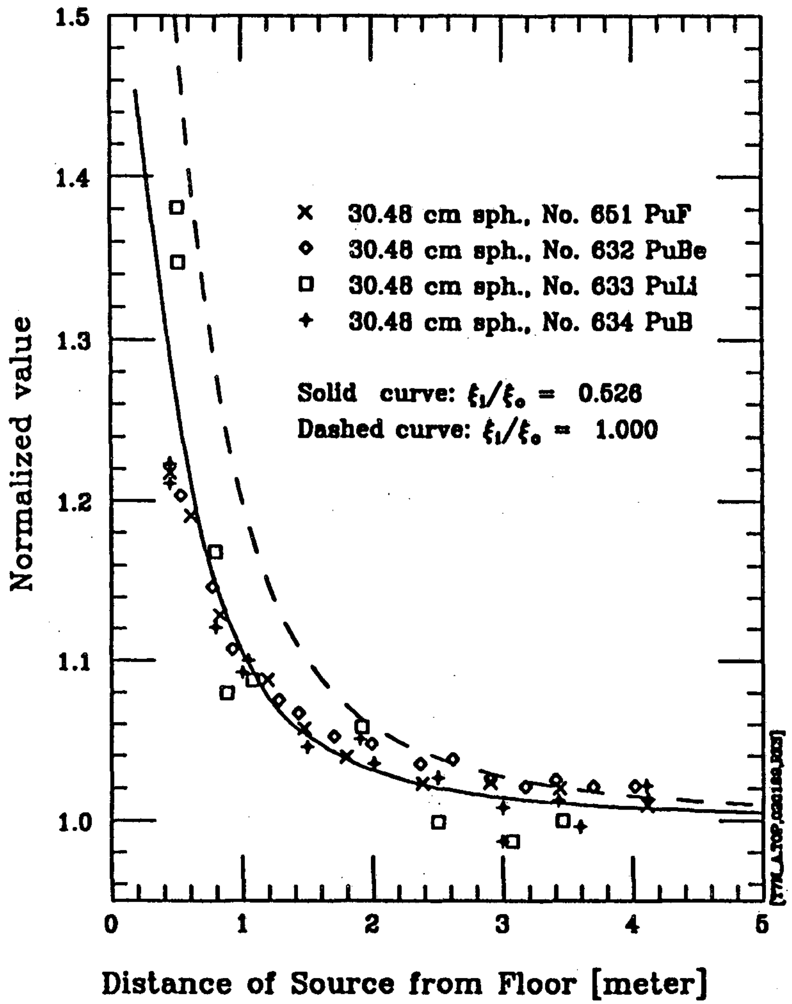

Fig. 11 Normalized scattering of neutrons for detector No. 7 (30.48 cm) and 4 sources (detector and source is 1 m apart and at the same height).

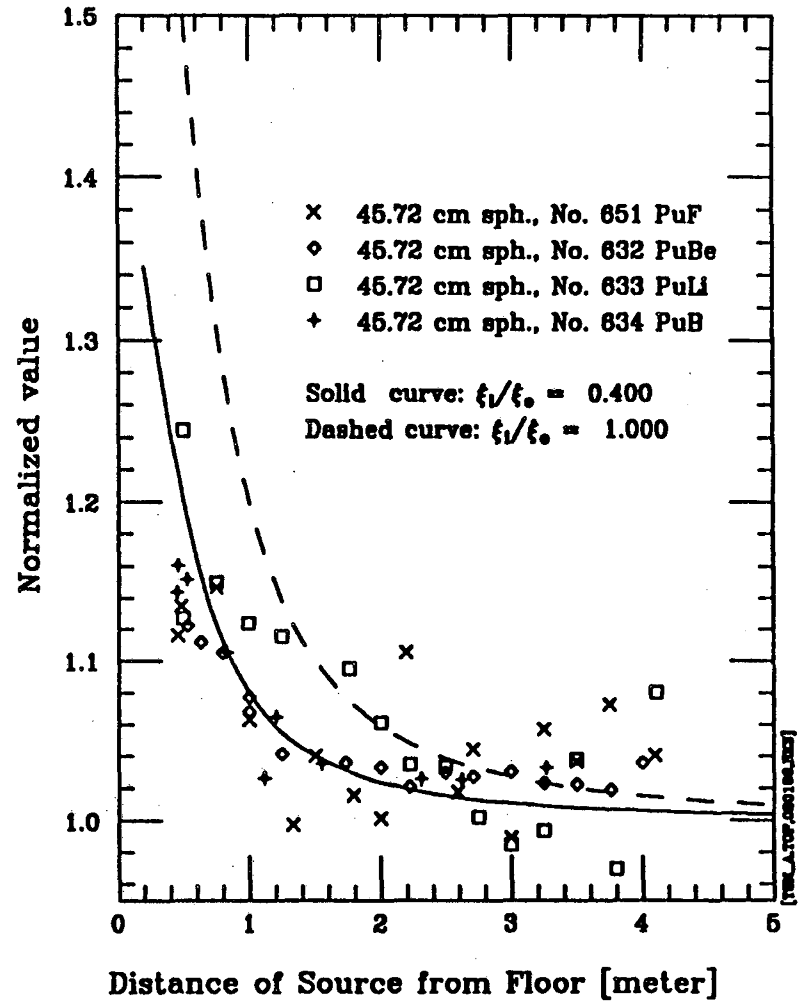

Fig. 12 Normalized scattering of neutrons for detector No. 8 (45.72 cm) and 4 sources (detector and source is 1 m apart and at the same height).

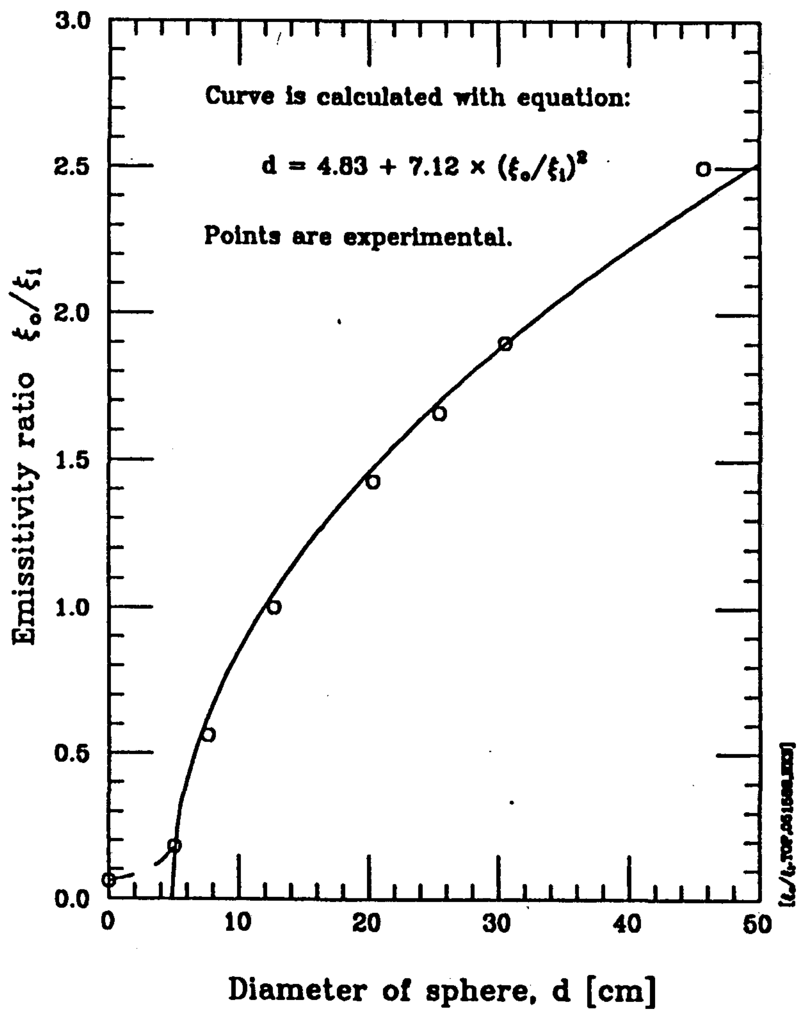

Fig. 13 Ratio of emissitivities, ξ_o to ξ_1, as functions of sphere diameter, d.